

**Direct Evidence for Modulated Irradiation
of Secondary Components in Dwarf Novae during Superoutbursts**

J. S m a k

N. Copernicus Astronomical Center, Polish Academy of Sciences,
Bartycka 18, 00-716 Warsaw, Poland
e-mail: jis@camk.edu.pl*Received*

ABSTRACT

Contribution from the irradiated secondary component is detected in the light curves of five dwarf novae observed during superoutbursts. Their superhump light curves show that irradiation is modulated with the superhump phase. This strengthens the new interpretation of superhumps (Smak 2009) as being due to the irradiation controlled mass transfer rate resulting in modulated dissipation of the kinetic energy of the stream.

Key words: *binaries: cataclysmic variables, – Stars: dwarf novae*

1. Introduction

From the analysis of the superoutburst light curves of four deeply eclipsing dwarf novae it was found (Smak 2009,2010) that the observed brightness of the disk is modulated with phase of the beat period. The amplitudes of this modulation and the phases of maximum obtained for the four systems were practically identical, their average values being: $\langle A \rangle = 0.18 \pm 0.01$ and $\langle \phi_b^{max} \rangle = 0.65 \pm 0.02$. Similar modulation was also detected in superhump amplitudes of six dwarf novae (Smak 2010), with values of ϕ_b^{max} being less accurate (0.62 ± 0.06 or 0.68 ± 0.08) but consistent with the original value. This was interpreted as being due to a non-axisymmetric structure of the disk, involving the azimuthal dependence of its geometrical thickness, rotating with the beat period.

Regardless of this interpretation it is obvious that modulation with the beat phase seen by the observer translates into modulated irradiation of the secondary component with the superhump phase. In particular, that the maximum irradiation of the secondary occurs at $\phi_{sh}^{max} = -\phi_b^{max} = 0.35 \pm 0.02$.

This became one of the crucial ingredients of the new interpretation of superhumps (Smak 2009) in terms of the irradiation controlled mass transfer rate resulting in modulated dissipation of the kinetic energy of the stream.

The purpose of this paper is to present results of an analysis of superoutburst light curves of five dwarf novae which provide *direct* evidence for the modulated irradiation of the secondary, thereby strengthening this interpretation. In Section 2 estimates are presented showing that the expected contribution from the irradiated secondary to the total brightness of the system should be detectable. The data and the methods of their analysis are described in Sections 3 and 4. In Section 5 the composite orbital light curves at superhump phases around ϕ_{sh}^{max} are presented showing the expected dependence on ϕ_{orb} . In Section 6 the composite superhump light curves near $\phi_{orb} = 0.5$ are compared to those near $\phi_{orb} = 0.0$, showing the expected modulation with ϕ_{sh} .

2. The Irradiated Secondary Component

We begin by estimating the expected contribution from the irradiated secondary to the total brightness of the system. To calculate its absolute visual magnitude we proceed as follows. The distribution of temperature over the irradiated hemisphere of the secondary is described by

$$\sigma T^4 = \frac{L_{BL}}{4 \pi D^2} \cos \theta, \quad (1)$$

where D is the distance from the primary to the point considered, θ is the incidence angle and

$$L_{BL} = \frac{1}{2} \frac{G M_1}{R_1} \dot{M} \quad (2)$$

is the luminosity of the boundary layer.

The absolute visual magnitude of the irradiated secondary is then calculated by integrating the emerging flux over its irradiated portion, i.e. excluding the equatorial parts which are in the shadow cast by the disk. The resulting magnitudes $M_{V,2}(\dot{M}, z/r)$ are functions of the accretion rate and of the disk thickness parameter z/r . Then the magnitudes of the system with and without irradiation are calculated, their difference $\Delta M_V(\dot{M}, z/r)$ giving the contribution from the irradiated secondary to the total brightness of the system. We adopt system parameters of Z Cha (Smak 2007), accretion rates between $\dot{M} = 1 \times 10^{17}$ and 3×10^{17} (as observed in Z Cha during its superoutbursts; Smak 2008a), and $z/r = 0.05 - 0.20$. The resulting values of ΔM_V depend primarily on z/r , ranging from $\Delta M_V \sim 0.45$ at $z/r = 0.05$ to $\Delta M_V \sim 0.25$ at $z/r = 0.20$.

3. The Data

The data to be used in our analysis, consisting of light curves of dwarf novae observed during their superoutbursts, were selected from the literature using two requirements: (1) a good coverage in orbital and superhump phases, and (2) the

superhump amplitudes larger than ~ 0.10 mag. Sufficient data were found for the following five stars:

OY Car. Light curves observed by Krzemiński and Vogt (1985; Fig.2b) on January 4-9, 1980, covering 17 superhumps.

Z Cha. Light curves observed during several superoutbursts by Warner and O'Donoghue (1988; Fig.1), with orbital phases of superhump maxima listed in their Table 3; regretfully, some of those phases are rather uncertain.

XZ Eri. Light curves observed by Uemura et al. (2004; Fig.2) on JD 2452668, 669, and 670, covering 8 superhumps.

VW Hyi. Three sets of data consist of light curves observed by Vogt (1974; Fig.5) on December 16-21, 1972; by Verbunt et al. (1987; Fig. 1); and by Schoembs and Vogt (1980; Fig.2a, Runs 1 and 2). VW Hyi is a non-eclipsing system, but its orbital period is well determined from "hot spot humps" observed at quiescence. We use the elements from van Amerongen et al. (1987) corrected by $\Delta\phi_{orb} = 0.15$ (Smith et al. 2006) accounting for the delay between the spectroscopic conjunction and the hump maximum.

DV UMa. Light curves observed by Patterson et al. (2000; Fig.4) on JD 2450553 and 554, covering 12 superhumps.

The data to be analysed in further sections consist of magnitudes read from the published light curves at specific superhump phases ϕ_{sh} (see Section 5) or at specific orbital phases ϕ_{orb} (see Section 6). In each case the corresponding orbital phase or superhump phase is also determined. In effect we have $m(\phi_{orb}, \phi_{sh})$. In addition, the magnitudes at maximum (m_{max}) and at minimum (m_{min}) of a given superhump cycle are obtained and used to determine the local values of the superhump amplitude: $A_{sh} = m_{min} - m_{max}$ and of the mean magnitude: $\langle m \rangle = (m_{min} + m_{max})/2$.

Prior to further analysis the observed light curves must be corrected for the presence of the "hot spot hump". In the case of Z Cha it was found (Smak 2007) that such a hump, with amplitude $A_{spot} \approx 0.15$ and maximum at $\phi_{orb}^{max} \approx 0.95$, is present when the corresponding beat phase $\phi_b = \phi_{orb} - \phi_{sh}$ is between ~ 0.3 and ~ 0.7 and absent at other beat phases; identical values of A_{spot} and ϕ_{orb}^{max} were obtained also for OY Car (Smak 2008b). Using this evidence we correct the observed magnitudes corresponding to $\phi_b = 0.3 - 0.7$ and – simultaneously – to $\phi_{orb} = 0.70 - 0.20$ by

$$\delta m_{spot} = 0.15 \cos(\phi_{orb} - 0.95). \quad (3)$$

It is known that the brightness of a dwarf nova and the amplitude of its superhumps decrease during superoutburst, showing also some additional variations. To compensate for those effects we define the reduced magnitudes as

$$\Delta m(\phi_{orb}, \phi_{sh}) = [m(\phi_{orb}, \phi_{sh}) - \langle m \rangle] \frac{\langle A_{sh} \rangle}{A_{sh}}, \quad (4)$$

where $\langle A_{sh} \rangle$ is the average superhump amplitude obtained from all data for a given star.

From considerations in the next Section it is clear that the effects of modulated irradiation of the secondary modify the shape of the entire superhump light curve including m_{min} and m_{max} . Consequently the values of $\Delta m(\phi_{orb}, \phi_{sh})$ are subject to uncertainties introduced by the use of the specific "prescription" defined by Eq.(4). We shall return to this problem in Section 6.

4. Qualitative Considerations

The observed brightness of an irradiated secondary depends on the orbital phase, with maximum at $\phi_{orb}^{max} = 0.5$, i.e. when its irradiated hemisphere is facing the observer. It also depends on the orbital inclination, with maximum effect to be seen at $i = 90^\circ$. On the other hand, according to the evidence already available (see Introduction), the irradiation is modulated with the superhump phase, with maximum at $\phi_{sh}^{max} \approx 0.35$.

If so, the effects of modulated irradiation should be visible in the observed light curves in the form of excess brightness near ϕ_{sh}^{max} when it coincides with $\phi_{orb} = 0.5$. Such an excess can actually be seen in some of the light curves. For example: in OY Car on January 7 and 8, 1980 (Krzemiński and Vogt 1985; Fig.2b), in Z Cha during run S2740 (Warner and O'Donoghue 1988; Fig.1), in XZ Eri on JD 2452668 and 669 (Uemura et al. 2004; Fig.2), and in DV UMa on JD 2450554 (Patterson et al. 2000; Fig.4).

The problem is, however, that irradiation effects can be seen in the *observed* light curves only selectively – in narrow intervals of phases. An obvious alternative is to construct *composite* light curves consisting of points corresponding to the specific orbital or superhump phases. Accordingly, we adopt the following two-step strategy for our analysis. First, in order to check whether the irradiation effects are really present and detectable, we will construct the *composite orbital* light curves using points with superhump phases near ϕ_{sh}^{max} . Secondly, in order to detect the effects of variable irradiation, we will construct the *composite superhump* light curves using points with orbital phases near $\phi_{orb} \sim 0.5$, i.e. close to the maximum irradiation, and compare them to the superhump light curves corresponding to $\phi_{orb} \sim 0.0$, i.e. to the phase where irradiation effects are absent.

5. The Orbital Light Curves – Detection of Irradiated Secondary

As discussed above the expected contribution from the irradiated secondary should be best seen in the composite orbital light curves corresponding to $\phi_{sh}^{max} \sim 0.35$. To account for the uncertainty of this value and to increase the number of points we construct the orbital light curves using $\Delta m(\phi_{orb}, 0.3)$ and $\Delta m(\phi_{orb}, 0.4)$.

The resulting *composite orbital* light curves for four stars are shown in Fig.1

(XZ Eri could not be included because of insufficient coverage in ϕ_{orb}). As can be seen, those light curves show the expected dependence on ϕ_{orb} quite clearly. The best fit cosine curves are shown in those figures mainly for illustrative purposes; in view of the large scatter and for reasons discussed in the next Section not much weight can be given to their parameters and for that reason they are not listed here.

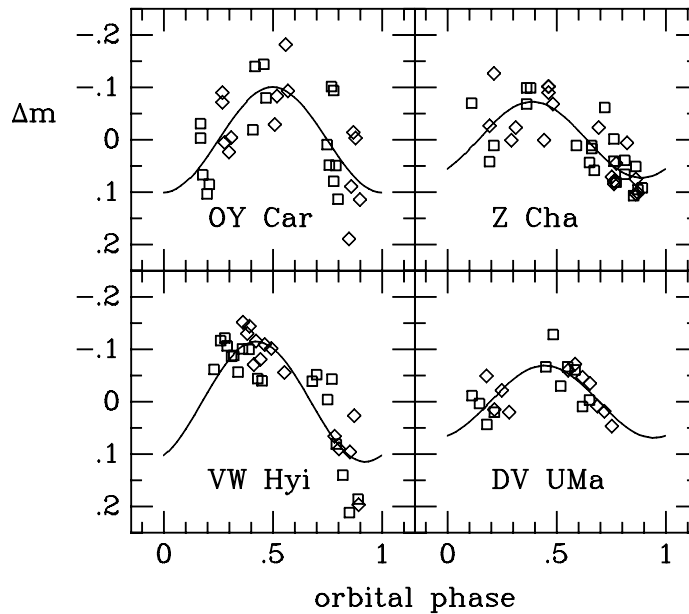


Fig. 1. The composite orbital light curves of four dwarf novae at $\phi_{sh} = 0.3$ (squares) and $\phi_{sh} = 0.4$ (diamonds). Best fit cosine curves are also shown.

There is one problem which requires comments. The light curves of high inclination systems should show a secondary eclipse near $\phi_{orb} = 0.5$ due to partial occultation of the secondary by the disk. It can be estimated, however, that the central depth of this eclipse is very low – comparable to the scatter of points in the light curves in Fig.1. To confirm those estimates we review the original light curves and find that such a very shallow eclipse is indeed present in only some of them: in the January 6, 1980, light curve of OY Car (Krzemiński and Vogt 1985; Fig.2b) and in the S0130 and S2740 light curves of Z Cha (Warner and O’Donoghue 1988; Fig.1).

6. The Superhump Light Curves – Detection of Modulated Irradiation

As suggested in Section 4 the expected contribution from the irradiated secondary should be best seen in the superhump light curve around $\phi_{orb} = 0.5$ and absent around $\phi_{orb} = 0.0$. Accordingly we determine the *composite superhump* light curves at $\phi_{orb} = 0.4, 0.5$ and 0.6 and at $\phi_{orb} = 0.9$ and 0.1 (for VW Hyi we

also use $\phi_{orb} = 0.0$).

Starting with superhump light curves near $\phi_{orb} = 0.0$, shown in Figs.2a-6a, we note that they are fairly smooth and can be fitted with a simple cosine shape:

$$\Delta m_{sh}^{\circ}(\phi_{sh}) = \Delta m_{\circ} + A_{sh} \cos \phi_{sh} . \quad (5)$$

Turning to superhump light curves near $\phi_{orb} = 0.5$, shown in Figs.2b-6b, we note that they differ systematically from those near $\phi_{orb} = 0.0$, showing the expected excess brightness around $\phi_{sh} \sim 0.5$. To show it more clearly we calculate the residuals

$$\delta m(0.4 - 0.6, \phi_{sh}) = \Delta m(0.4 - 0.6, \phi_{sh}) - \Delta m_{sh}^{\circ}(\phi_{sh}) , \quad (6)$$

where $\Delta m_{sh}^{\circ}(\phi_{sh})$ is given by Eq.5.

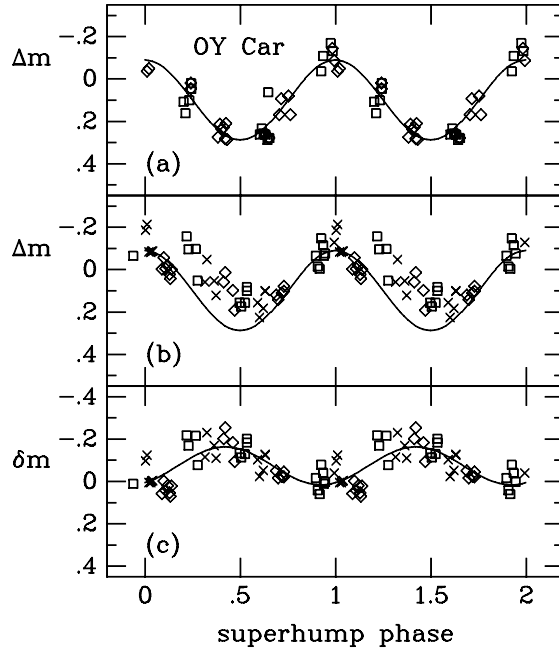


Fig. 2. (a) The composite superhump light curve of OY Car at $\phi_{orb} = 0.1$ (squares) and $\phi_{orb} = 0.9$ (diamonds). Solid line is the best fit cosine curve. (b) The composite superhump light curve of OY Car at $\phi_{orb} = 0.4$ (squares), $\phi_{orb} = 0.5$ (crosses) and $\phi_{orb} = 0.6$ (diamonds). Solid line is the same as in (a). (c) The residuals (see Eq.6) between points in (b) and the best fit cosine curve. Symbols are the same as in (b). Solid line is the best fit cosine curve representing the residuals.

Those residuals, plotted in Figs.2c-6c, clearly show the expected modulation with ϕ_{sh} . Shown also are the best fit cosine curves, their parameters A_{irr} and ϕ_{sh}^{max} being listed in Table 1.

The case of Z Cha requires special comment. Fig.3b shows peculiar distribution of points near $\phi_{sh} = 0.0$. This is most likely due to very narrow shapes of some of

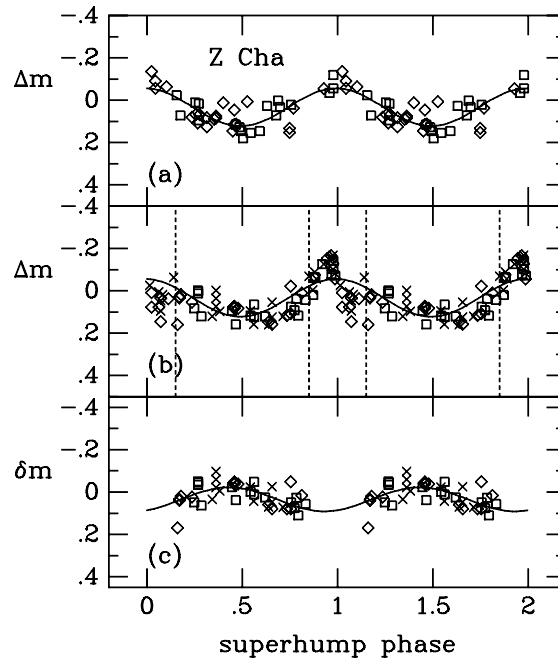


Fig. 3. The composite superhump light curves of Z Cha. For explanations – see caption to Fig.2. Dotted lines in (b) show the interval of phases not used in the analysis of residuals shown in (c). See text for details.

Table 1
Parameters of Modulated Irradiation

Star	A_{irr}	ϕ_{sh}^{max}
OY Car	0.09 ± 0.02	0.42 ± 0.03
Z Cha	0.06 ± 0.02	0.43 ± 0.04
XZ Eri	0.08 ± 0.02	0.60 ± 0.04
VW Hyi	0.10 ± 0.01	0.51 ± 0.02
DV UMa	0.15 ± 0.02	0.50 ± 0.02

the superhumps and uncertain phases of their maxima. Rather than arbitrarily modifying those points we simply exclude them from the analysis of residuals shown in Fig.3c.

We now return to the problem of uncertainties related to the use of the specific form of Eq.(4) adopted in Section 3. To clarify this point we repeated our analysis

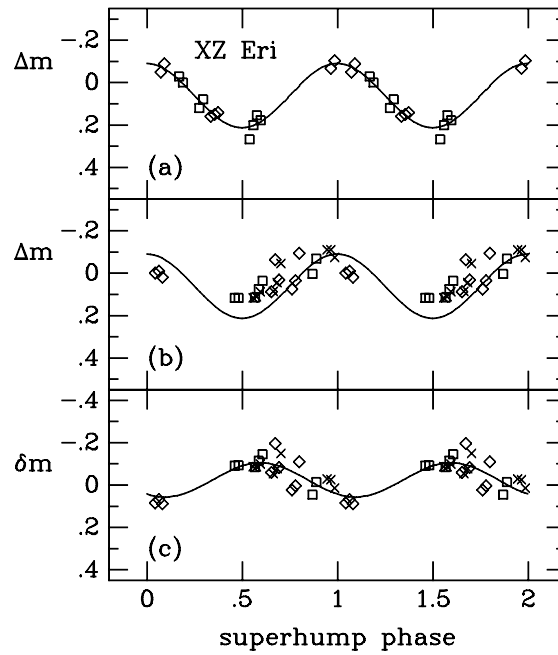


Fig. 4. The composite superhump light curves of XZ Eri. For explanations – see caption to Fig.2.

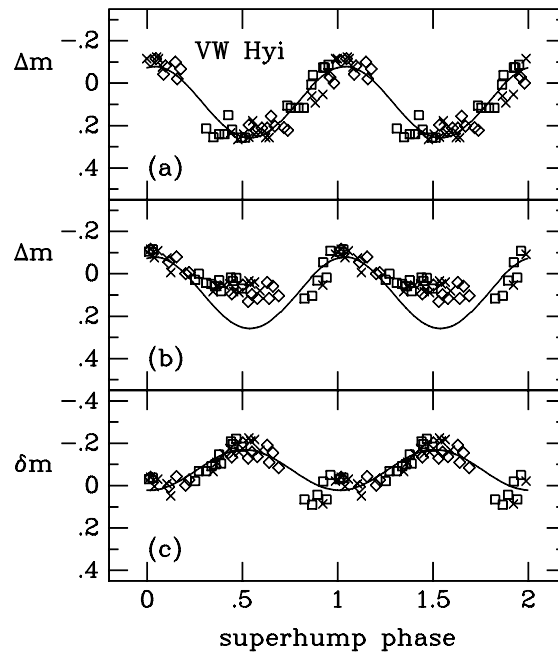


Fig. 5. The composite superhump light curves of VW Hyi. Crosses in (a) correspond to $\phi_{orb} = 0.0$. For other explanations – see caption to Fig.2.

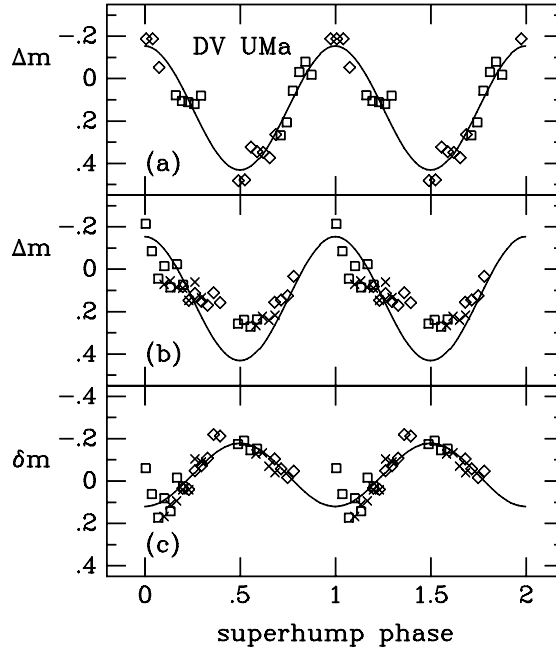


Fig. 6. The composite superhump light curves of DV UMa. For explanations – see caption to Fig.2.

using two alternative versions of this equation, with $\langle m \rangle$ being replaced by m_{min} or m_{max} , and its three other versions without factor $\langle A_{sh} \rangle / A_{sh}$. Results were *qualitatively* the same, showing clearly the effects of modulated irradiation. As could be expected, however, the amplitudes A_{irr} turned out to be sensitive to the particular form of Eq.(4); therefore their values listed in Table 1 should not be given much weight. On the other hand, the phases of maximum ϕ_{sh}^{max} depend only slightly on the particular form of Eq.(4).

7. Conclusions

The composite superhump light curves presented in Section 6 clearly show that the irradiation of the secondary component is modulated with the superhump phase. Subject to uncertainties discussed in that Section, the full amplitude of those variations $\langle 2A_{irr} \rangle \approx 0.2$ mag (which is actually the difference between maximum and minimum irradiation) is consistent with estimates presented in Section 2.

The mean phase of maximum irradiation $\langle \phi_{sh}^{max} \rangle = 0.49 \pm 0.03$ for the five stars listed in Table 1 differs from $\langle \phi_{sh}^{max} \rangle = 0.35 \pm 0.02$ obtained earlier from indirect evidence (see Introduction). The origin of this difference is quite obvious: the value $\langle \phi_{sh}^{max} \rangle = 0.35$ refers to the moment of maximum irradiation, while $\langle \phi_{sh}^{max} \rangle = 0.49$ – to the moment when its consequences show up in the light curve. In other words – the difference $\Delta\phi_{sh} \approx 0.14$ represents the response time of the atmospheric layers to variable irradiation. Model calculations by Hameury et

al. (1988, Fig.1) show that the transition from the initial state without irradiation to the state when a hot isothermal layer extends to sub-photospheric layers occurs on a time scale longer than $\Delta t \sim 10^3$ s. Once such a layer is formed, however, its response time to variable irradiation becomes shorter. In our case we have: $\Delta t = \Delta\phi_{sh}P_{sh} \approx 900$ s.

REFERENCES

- Hameury, J.M., King, A.R., Lasota, J.P. 1988, *A&A*, **192**, 187.
Krzemiński, W. and Vogt, N. 1985, *A&A*, **144**, 124.
Patterson, J., Vanmunster, T., Skillman, D.R., Jensen, L., Stull, J., Martin, B., Cook, L.M., Kemp, J., Knigge, C. 2000, *PASP*, **112**, 1584.
Schoembs, R. and Vogt, N. 1980, *A&A*, **91**, 25.
Smak, J. 2007, *Acta Astron.*, **57**, 87.
Smak, J. 2008a, *Acta Astron.*, **58**, 55.
Smak, J. 2008b, *Acta Astron.*, **58**, 65.
Smak, J. 2009, *Acta Astron.*, **59**, 121.
Smak, J. 2010, *Acta Astron.*, **60**, 357.
Smith, A.J., Haswell, C.A., Hynes, R.I. 2006, *MNRAS*, **369**, 1537.
Uemura, M. et al. 2004, *Publ.Astr.Soc.Japan*, **56**, S141.
van Amerongen, S., Damen, E., Groot, M., Kraakman, H., van Paradijs, J. 1987, *MNRAS*, **225**, 93.
Verbunt, F., Hassall, B.J.M., Pringle, J.E., Warner, B., Marang, F. 1987, *MNRAS*, **225**, 113.
Vogt, N. 1974, *A&A*, **36**, 369.
Warner, B. and O'Donoghue, D. 1988, *MNRAS*, **233**, 705.